Proc. of the X Int. Conf. — Ion Implantation and other Applications of Ions and Electrons, Kazimierz Dolny 2014

Response of ZnO/GaN Heterostructure to Ion Irradiation

A. Barcz[a,b], K. Pągowska[a,*], M. Kozubal[a], E. Guziewicz[b], M.A. Borysiewicz[a], J. Dyczewski[b], R. Jakieła[b], J. Ratajczak[a], D. Snigurenko[b] and E. Dynowska[a,b]

[a]Institute of Electron Technology, al. Lotników 32/46, 02-668 Warsaw, Poland

[b]Institute of Physics, Polish Academy of Sciences, al. Lotników 32/46, 02-668 Warsaw, Poland

In this paper we report on the analysis of Al^+-implanted ZnO/GaN bilayers in search for the damage production mechanism and possible ion mixing. 100 nm or 200 nm thick ZnO epitaxial layers were grown on GaN substrates by either sputter deposition or atomic layer deposition technique followed by adequate annealing. Ion irradiations of ZnO/GaN were carried out at room temperature using 200 keV Al^+ ions with fluences of 2×10^{15} and 10^{16} at./cm^2. Unprocessed and irradiated samples were characterized by the Rutherford backscattering spectrometry in channeling geometry (RBS\c), X-ray diffraction and transmission electron microscopy. Additionally, secondary ion mass spectrometry was employed for the aforementioned samples as well as for the implanted samples subjected to further annealing. It was found that the damage distributions in ZnO/GaN differ considerably from the corresponding defect profiles in the bulk ZnO and GaN crystals, most probably due to an additional strain originating from the lattice mismatch. Amount of intermixing appears to be relatively small; apparently, efficient recombination prevents foreign atoms to relocate to large distances.

DOI: 10.12693/APhysPolA.128.832

PACS: 61.82.Fk, 61.85+p, 68.35.Dv

1. Introduction

ZnO and GaN are important wide band-gap semiconductor materials, to some extent similar in terms of material properties [1]. Both ZnO and GaN have a wurtzite crystal structure, nearly the same in-plane lattice parameter (the lattice mismatch ≈1.8%) and room-temperature band-gap energy of 3.3 eV and 3.4 eV, respectively [2].

In recent years, the growth of GaN–ZnO heterostructures has attracted much attention. This may be in particular due to a feasibility to realize a p–n junction in planar or coaxial form for nano-photonics and nano-electronics applications because of the much better p-doping properties of GaN as compared to ZnO [3]. In addition, ZnO and GaN can form solid solutions [4] which, in principle, should enhance ion mixing. While GaN based light emitting diodes and laser are already realized on an industrial scale, ZnO still suffers from several problems, in particular, a lack of efficient and reproducible p-type doping [5].

Another common feature of both semiconductors is their strong resistance to radiation damage [6]. This is an important characteristic for device processing steps involving ion implantation, for example for doping or isolation and for the use of electronic circuits in radiation environments, such as in space or nuclear reactors.

In the fabrication of ZnO- and III-nitride-based devices, ion bombardment represents an attractive processing tool for several technological steps, including selective doping, electrical isolation and ion slicing. High resistance to radiation damage of ZnO and GaN is due to the efficient dynamic annealing of defects that occur during irradiation. Due to extremely efficient dynamic annealing in ZnO, the ion doses needed for isolation of this material are about 2 orders of magnitude larger than the corresponding ones in the case of another wide band-gap semiconductor, GaN [7].

Ion mixing is a processing technique for the fabrication of new materials with unique properties [8]. Ion-induced mixing can not only lead to stable compound formation, but also to metastable alloy formation. The process involves bombardment of the layered sample with doses sufficient to induce mixing at the interface, and generally serves as a means of preparing electrical junctions, especially between non-equilibrium or metastable alloys and intermetallic compounds. Materials get mixed when energetic ions travelling through their interface produce mutual relocation of the constituents from both sides.

The aim of this work is to compare the degree of ion-damage in ZnO/GaN bilayer relative to the bulk compounds and to evaluate the extent of intermixing.

2. Experimental

For ZnO growth we used the atomic layer deposition (ALD) method which is a variant of the chemical vapor deposition (CVD) technique. The main characteristic feature of the ALD process is a sequential deposition procedure. ALD is based on the surface chemical reaction between two reagents (here called "precursors") that are alternatively introduced into a growth chamber. The pulses of precursors are interrupted by purging with an inert gas, which prevents chemical reactions inside the reaction chamber as precursors react only at the surface of the growing film. Therefore highly reactive precursors can be applied and, consequently, deposition temperature can be quite low.

*corresponding author; e-mail: pagowska@ite.waw.pl

For the present study we used diethylzinc (DEZn) and deionized water as zinc and oxygen precursors, respectively. Zinc oxide was created as a result of a double-exchange chemical reaction that took place at the surface

$$Zn(C_2H_5)_2 + H_2O \rightarrow ZnO + 2C_2H_6. \quad (1)$$

The growth processes were performed using the BENEQ TSF-200 reactor. Films were deposited at the temperatures in the range of 280–320 °C. As substrates we used commercial GaN/Al_2O_3 templates with the 2 µm thick GaN layer [9, 10].

Additionally, we prepared ZnO thin films, deposited by means of RF magnetron sputtering using a 3" 4N-pure ZnO target based on a previously developed approach [11]. However, the analysis of this samples did not depart significantly from those included to this paper.

The TRIM code [12] was employed to simulate the implanted ions and deposited energy distributions, as depicted in Fig. 1.

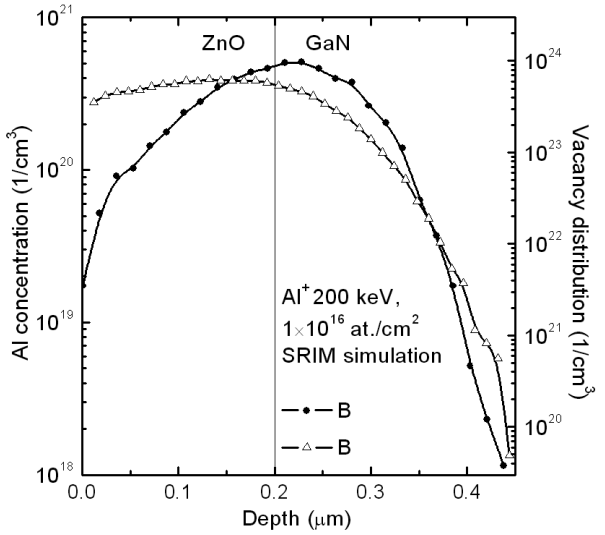

Fig. 1. Al depth profile and vacancy distribution, computed using the stopping and range of ions in matter (SRIM) simulation.

Implantations with 200 keV Al^+ ions with the fluences of 2×10^{15} and 10^{16} at./cm^2 were performed at RT in the NEC 3SDH-2 Pelletron Accelerator. The aforementioned accelerator was further employed for the analysis of virgin and implanted samples with the Rutherford backscattering spectroscopy in channeling geometry (RBS/c) using 2 MeV $^4He^{++}$ beam.

Thermal treatment of the samples was conducted in a quartz furnace at 900 °C in Ar atmosphere or at 800 °C in air, both for 1/2 hour.

Transmission electron microscope investigations were carried out using a JEOL JEM 2100 scanning-transmission electron microscope operating at 200 keV. It is a high resolution (0.14 nm planar resolution) microscope (HRTEM) with a LaB6 emitter, equipped with X-ray energy dispersive spectrometer, bright field detector and dark field detector enabling high angle annular dark field observations (HAADF) in the scanning transmission mode of operation. Samples for TEM observations were prepared as cross-sectional ones, mostly in a focused ion beam microscope (Helios NANOLAB). In order to obtain high quality specimens, deprived of any preparation damages, necessary for atomic planes imaging, specimens were additionally cleaned in argon ion millers.

The X-ray measurements were performed with the use of X-ray diffractometer X'Pert PRO MPD Panalytical configured for the Bragg–Brentano diffraction geometry, equipped with a strip detector, an incident-beam Johansson monochromator and Cu K_{α_1} radiation.

SIMS measurements were conducted using a CAMECA IMS6F device operating with caesium (Cs^+) primary beam, with the current kept at 100 nA.

3. Results and discussion

3.1. XRD

The diffractogram (Fig. 2) shows a distinct 00.2 and 00.4 peak pairs for ZnO and GaN films. This feature, especially visible for a close-up near 00.4 GaN peak in Fig. 2b, is a proof of a relatively good crystalline quality of those layers (in agreement with RBS\c). In the opposite case, 00.4 ZnO peak would not be distinguishable

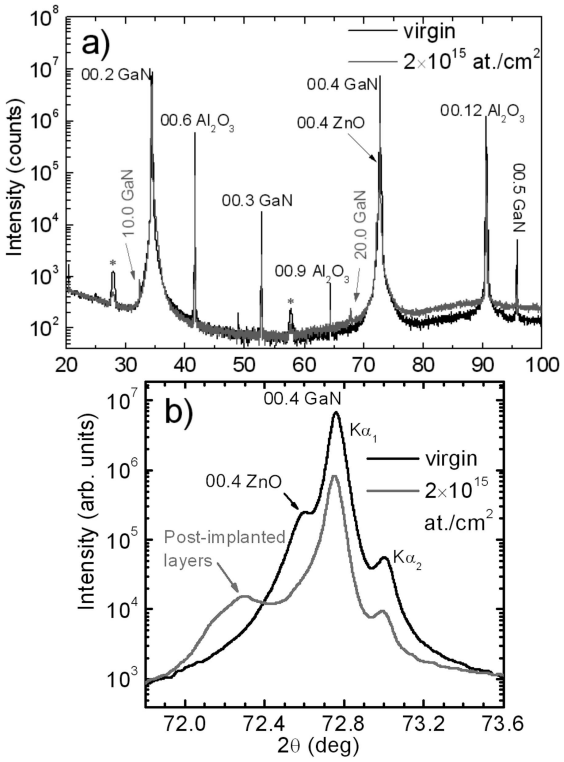

Fig. 2. X-ray diffraction patterns of as grown $ZnO/GaN/Al_2O_3$ sample. Part a) concerns untreated (black) and implanted with 200 keV 2×10^{15}Al/cm^2 (gray). Part b) displays the comparison of the X-ray diffraction patterns in the vicinity of 00.4 GaN reflection of as grown with Al^+ implanted $ZnO/GaN/Al_2O_3$ samples.

from 00.4 GaN one (because of very similar lattice parameters).

Two results of Al^+ irradiation are presented in Fig. 2b — significant 00.4 ZnO peak decrease as well as the emergence of a signal at the lower angles than for both 00.4 GaN and 00.4 ZnO. It originates from the damaged layer with the lattice parameter larger than that for GaN and ZnO.

3.2. TEM

To get detailed insight into structural transformations, TEM analysis has been performed, showing columnar structure of the ZnO layer on single crystal GaN as well as the interface between them. Micrograph for bombarded ZnO/GaN sample (Fig. 3b) presents structural deterioration (porous layer, microvoids) as compared to the untreated one, Fig. 3a.

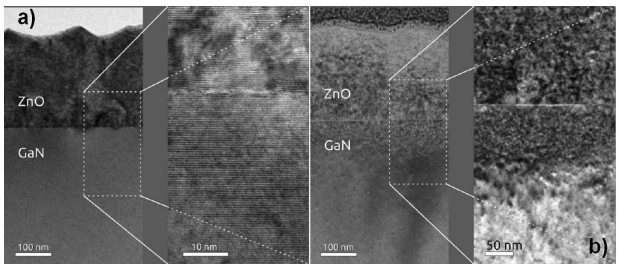

Fig. 3. TEM micrograph for ZnO/GaN epilayer, a) unimplanted and b) irradiated with 200 keV 10^{16}Al/cm^2.

3.3. RBS\c

Figure 4a shows random and aligned spectra for 200 nm thick ZnO/GaN epilayers subjected to implantations with different fluences. Zn and Ga signals overlap and thus are visible as one peak. As expected, with increasing Al fluence the whole spectrum increases monotonically due to the progressing damage build-up in ZnO/GaN layer. Similar behaviour occurs for bulk ZnO specimen, Fig. 4b. One additional characteristic feature also stands out — formation of a distinct band in the 1300–1500 keV energy range, which corresponds to the damage caused by implantation. Channeling spectra measured along [00.1] axis for virgin samples revealed a very low channeling minimum yield — $\chi_{\min} = 4.2\%$.

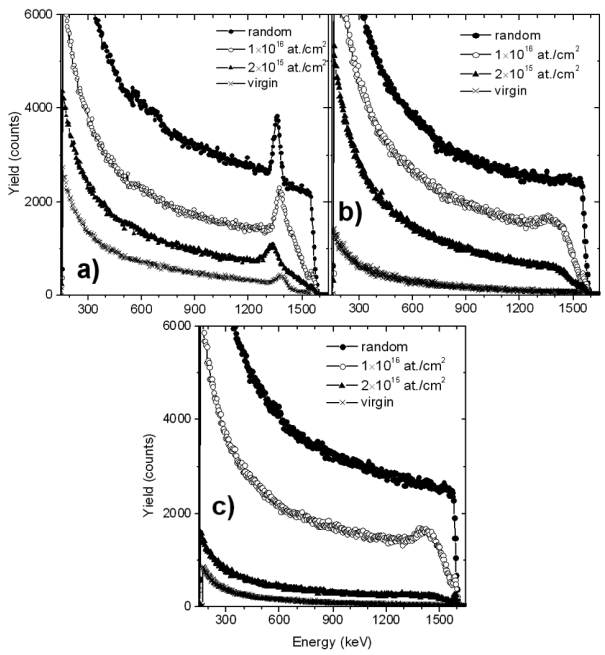

Fig. 4. Random and aligned RBS spectra measured at 2 MeV $^4He^{++}$ beam for a) 200 nm thick ZnO/GaN epilayer, b) bulk ZnO, subjected to the implantation with different fluences with 200 keV Al^+ ions and c) bulk GaN, subjected to the implantation with different fluences with 200 keV Al^+ ions.

3.4. SIMS

SIMS analyses showed that the unimplanted ZnO/GaN heterostructure remains stable at 800 °C. The Al implantation with a higher fluence followed by annealing at 800 °C leads to a complete exfoliation of the ZnO film.

4. Conclusions

The presented results allow us to formulate some conclusions on the nature of damage build-up in ion bombarded GaN, ZnO and their combination. First of all, let us notice that the non-perfect crystallographic quality of the as-deposited ZnO films did not deviate from the analogous structures obtained in other laboratories. Fortunately, the observed morphology with single crystalline columns oriented along the *c* axis allows one to effectively apply ion channeling as a tool to evaluate the effect of damage evolution. The difference in the defect concentration found between the irradiated ZnO/GaN vs. bulk GaN or ZnO may arise from additional strain caused by the lattice mismatch of the two materials. The extent of intermixing appears to be relatively small; apparently, efficient recombination prevents foreign atoms to relocate to large distances. The above situation illustrates a typical conflict between thermodynamic and kinetic considerations — even if energetically ZnO and GaN may form solid solutions, mutual injection of atoms from one crystal to another is impeded by rapid annihilation of defects taking place within the collision cascades. Nevertheless, the Al irradiation must have affected the constitution of the ZnO–GaN interface as the annealing of the implanted structure does lead to the exfoliation of the ZnO overlayer while the same annealing of the as-grown structure does not. The work is to be continued with a reversed bilayer — a gallium nitride grown by molecular beam epitaxy on a single crystal bulk zinc oxide.

Acknowledgments

This work was financed in the frames of ITE statutory activities.

References

[1] Y. Chen, D.M. Bagnal, H.J. Koh, K.T. Park, K. Hiraga, Z. Zhu, T. Yao, *J. Appl. Phys.* **84**, 3912 (1998).

[2] Ya.I. Alivov, J.E. Van Nostrand, D.C. Look, M.V. Chukichev, B.M. Ataev, *Appl. Phys. Lett.* **83**, 2934 (2003).

[3] S.B. Thapa, *Annual Report Institute of Optoelectronic Ulm University*, 2007, p. 79.

[4] J. Wang, B. Huang, Z. Wang, P. Wang, H. Cheng, Z. Zheng, X. Qin, X. Zhang, Y. Dai, M-H. Whangbo, *J. Mater. Chem.* **21**, 4562 (2011).

[5] K. Lorenz, E. Wendler, in: *Ion Implantation*, Ed. M. Goorsky, InTech, Rijeka 2012.

[6] S.O. Kucheyev, J.S. Williams, C. Jagadish, *Vacuum* **73**, 93 (2004).

[7] S.O. Kucheyev, P.N.K. Deenapanray, C. Jagadish, J.S. Williams, M. Yano, K. Koike, S. Sasa, M. Inoue, K.-I. Ogata, *Appl. Phys. Lett.* **81**, 3350 (2002).

[8] S. Matteson, M-A. Nicolet, *Ann. Rev. Mater. Sci.* **13**, 339 (1983).

[9] E. Guziewicz, M. Godlewski, L. Wachnicki, T.A. Krajewski, G. Luka, S. Gieraltowska, R. Jakiela, A. Stonert, W. Lisowski, M. Krawczyk, J.W. Sobczak, A. Jablonski, *Semicond. Sci. Techn.* **27**, 074011 (2012).

[10] I.A. Kowalik, E. Guziewicz, K. Kopalko, S. Yatsunenko, M. Godlewski, A. Wójcik, V. Osinniy, T. Krajewski, T. Story, E. Łusakowska, W. Paszkowicz, *Acta Phys. Pol. A* **112**, 401 (2007).

[11] M.A. Borysiewicz, I. Pasternak, E. Dynowska, R. Jakieła, V. Kolkovski, A. Dużyńska, E. Kamińska, A. Piotrowska, *Acta Phys. Pol. A* **119**, 686 (2011).

[12] J.F. Ziegler, M.D. Ziegler, J.P. Biersack, *Nucl. Instrum. Methods Phys. Res. B Beam Interact. Mater. At.* **268**, 1818 (2010).